TRIGGERLESS READOUT WITH TIME AND AMPLITUDE RECONSTRUCTION OF EVENT BASED ON DECONVOLUTION ALGORITHM*

Szymon Kulis†, Marek Idzik

Faculty of Physics and Applied Computer Science
AGH — University of Science and Technology
Mickiewicza 30, 30-059 Kraków, Poland

(Received January 31, 2011)

In future linear colliders like CLIC, where the period between the bunch crossings is in a sub-nanoseconds range (~ 500 ps), an appropriate detection technique with triggerless signal processing is needed. In this work we discuss a technique, based on deconvolution algorithm, suitable for time and amplitude reconstruction of an event. In the implemented method the output of a relatively slow shaper (many bunch crossing periods) is sampled and digitalised in an ADC and then the deconvolution procedure is applied to digital data. The time of an event can be found with a precision of few percent of sampling time. The signal to noise ratio is only slightly decreased after passing through the deconvolution filter. The performed theoretical and Monte Carlo studies are confirmed by the results of preliminary measurements obtained with the dedicated system comprising of radiation source, silicon sensor, front–end electronics, ADC and further digital processing implemented on a PC computer.

DOI:10.5506/APhysPolBSupp.4.49
PACS numbers: 29.85.–c, 29.85.Ca, 29.28.Fj

1. Introduction

The detectors in the Compact Linear Collider (CLIC) at CERN [1] and other future experiments, for which no external event trigger is foreseen, require a triggerless readout electronics with good time and amplitude resolution and with high pileup rejection capabilities. In addition, for dense multichannel systems, a small area and a low power consumption are among the key requirements to be satisfied. Such requirements lead usually to the

* Presented at the Workshop on Timing Detectors, Kraków, Poland, November 29–December 1, 2010.
† Corresponding author: kulis@fatcat.ftj.agh.edu.pl

need of dedicated VLSI multichannel readout electronics. The works are ongoing on development of such readout electronics for the luminosity detector (LumiCal) at CLIC. The LumiCal design results in about 200 000 channels to be readout. Each channel should measure the event amplitude with 8–10 bit accuracy [2] and the time of event with a precision of 5–10 ns.

In the systems, where the time and amplitude information is required, the most popular readout architecture is a dual chain scheme. One fast chain is used for timing information and a second, slower one, for the amplitude. An attractive possibility would be to use only one processing chain (Fig. 1), with an ADC incorporated in each channel, for both the amplitude and time measurement and to take an advantage of today's high performance low power digital technology, moving the signal processing to digital domain at the earliest possible stage.

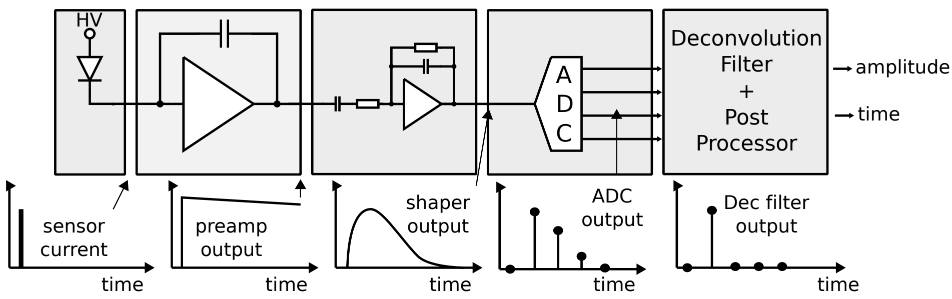

Fig. 1. Block diagram of proposed readout scheme.

The aim of this work is to verify performance of the deconvolution based readout architecture for the LumiCal detector. In Sec. 2 the theoretical principles and properties of the deconvolution filter are introduced. In Sec. 3 we describe a dedicated setup built to verify experimentally the deconvolution performance. In Sec. 4 we show the preliminary results of measurements together with the results of the Monte Carlo simulations.

2. Deconvolution

The pulse at front–end electronics output is a convolution of the sensor input signal and the front–end impulse response. Sampling and digitising the pulse with continuously running ADC and taking advantage of a known pulse shape one can perform an invert procedure — the deconvolution — to get the information about the time and amplitude of an event.

The deconvolution idea was proposed for the use in pulse shaping in HEP experiments at the beginning of 90s [3]. It was then implemented in different versions of APVs (analog pipeline voltage) ASICs designed for experiments synchronous with beam like CMS at LHC, where the deconvolution was performed by analog pulse shape processor (APSP) [4]. The main goal was the amplitude measurement with good pileup rejection plus a rough estimation of time (to identify the beam crossing repeating every 25 ns).

In this work we apply the deconvolution principle in asynchronous systems to obtain precise timing information in a few ns range, in addition to good signal to noise (SNR) ratio and pileup rejection. The analog part of readout chain should be kept as simple as possible and in addition the deconvolution procedure should not be complicated. A traditional CR-RC shaping fulfils these requirements.

For delta like signal in a sensor a semi-Gaussian response

$$V_{\rm sh}(s) = \frac{1}{(s+1/\tau)^2}$$

with the time constant τ, is obtained at the output of CR-RC shaper. To reconstruct the original sensor signal a deconvolution filter with transfer function

$$D(s) = \frac{1}{V_{\rm sh}(s)} = (s+1/\tau)^2 \tag{1}$$

needs to be applied. The discrete time implementation of such filter in digital domain may be obtained using the Z transform. Using the pole-zero mapping, each pole or zero (in the S plane) is replaced by its mapped z position according to $z = e^{sT_{\rm smp}}$, where $T_{\rm smp}$ is the sampling period. Then formula (1) transforms to

$$D(z) = 1 - 2e^{-T_{\rm smp}/\tau}z^{-1} + e^{-2T_{\rm smp}/\tau}z^{-2}\,, \tag{2}$$

where z^{-1} is a unit delay. From (2) the expression for deconvolution filtering in time domain is obtained

$$d(t_i) = Z^{-1}\left(D(z)\right) = V_{\rm sh}(t_i) - 2e^{-T_{\rm smp}/\tau}V_{\rm sh}(t_{i-1}) + e^{-2T_{\rm smp}/\tau}V_{\rm sh}(t_{i-2})\,. \tag{3}$$

It may be noticed that the deconvolution filter is very light, requiring only two multiplications and three additions. In Fig. 2 an example response (dots) of the deconvolution filter to sampled (squares) shaper output is shown.

The deconvolution procedure produces only one non-zero sample (Fig. 2, left) with amplitude proportional to the input pulse. This is the case only when the input pulse is synchronised with sampling clock. In any other case the filter produces two non-zero samples (Fig. 2, right). The ratio of these samples depends on phase difference between the input pulse and sampling clock. Since this ratio is a monotonic function of the phase shift it can be used to find the time of input pulse. The amplitude of input pulse can be

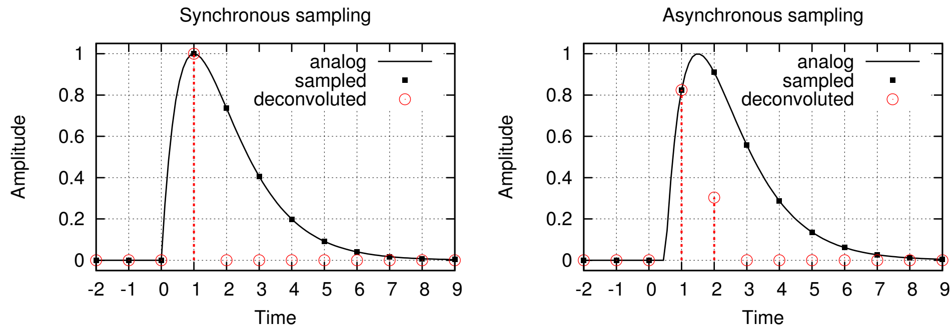

Fig. 2. Deconvolution filter response ($T_{\mathrm{smp}} = T_{\mathrm{peak}} = 1$, amp $= 1$). Pulse (left) synchronous and (right) asynchronous with sampling clock.

found from the sum of two non-zero samples multiplied by a time depended correction factor. All these operations can be done using the look-up tables, possibly offline.

The deconvolution method has very good pileup rejection capabilities. In Fig. 3 (left) an example with two events distant 2.1 T_{smp} is shown. Since there is one zero sample between the pulses after the deconvolution the events can be fully resolved.

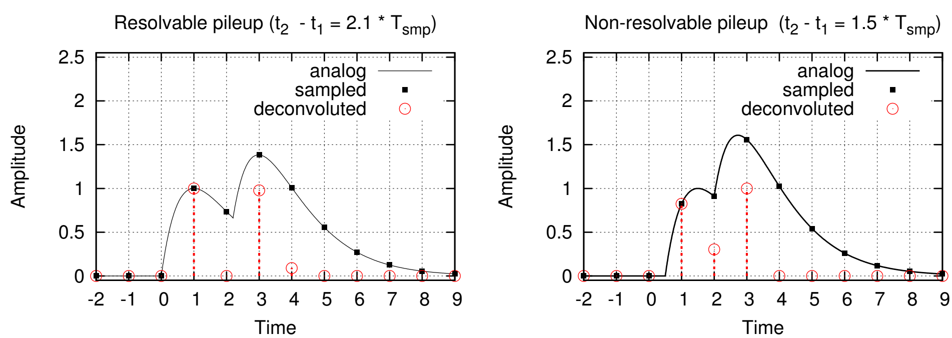

Fig. 3. Response of the deconvolution filter to (left) resolvable and (right) non-resolvable pileuped events ($T_{\mathrm{smp}} = T_{\mathrm{peak}} = 1$, amp $= 1$).

In general, the time separation must be grater than 2–3 T_{smp} (depending on the phase difference) for unambiguous deconvolution. In Fig. 3 (right) a non resolvable pileup is presented. Nevertheless, even in this case the deconvolution gives signature of more than two non-zero subsequent samples which can be used to reject those events.

3. Experimental setup

In order to verify the deconvolution based readout in a real experiment environment, a dedicated experimental setup was built (Fig. 4). The detection system contains a silicon sensor followed by a dedicated front–end electronics and a commercial ADC. As a radiation sensor a standard 300 μm (p+ on n) silicon diode is used. The front–end electronics used in this work is the one developed for the LumiCal detector at ILC [5]. It consists of a charge sensitive preamplifier followed by a first order CR-RC shaper with fixed peaking time of 60 ns. The measured Signal-to-Noise ratio of such sensor plus front–end chain is about 20 for the Minimal Ionising Particle (MIP).

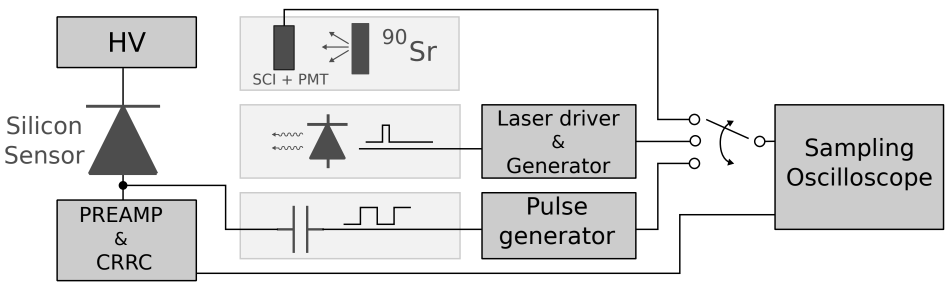

Fig. 4. Measurement setup diagram.

The output of the front–end is sent to a very fast sampling oscilloscope (MSO7104B 4 Gs/s) which is used as an ADC.

To generate an event three different operation modes are used. In the first mode a pulse from a pulse generator is sent to the front–end input. In this mode a very precise time reference is available but the whole readout chain is not tested because the sensor is not used. The second mode uses a radioactive β-source and the photo-multipliers are used for time reference. In this case the whole readout chain is tested but the time reference is not very precise because of the time uncertainty related to the response of the photo-multipliers. As the other disadvantage the electrons from β-source have a relatively low energy causing that the time of flight cannot be neglected. Finally, there is not a precise information about the pulse amplitude which could be used to benchmark the deconvolution algorithms. The most valuable, third mode, uses a laser diode. In this mode very short ($\sim$ 100 ps) infra-red laser pulses, with constant amplitude and a very precise timing information (provided by the laser driver), are generated. For these reasons the measurements performed with laser source are considered to be the most precise ones.

A dedicated software framework was developed. It can be divided into three modules: the acquisition, the Monte Carlo simulations and the data analyses. The acquisition part allows to collect data from ADC. The MC simulation module is used to generate pulses with given shape and with given noise spectrum [6]. The same data analyses procedures are used for the measurement and MC simulation data to benchmark the applied deconvolution algorithms.

4. Measurement and MC simulations results

In Fig. 5 (left) the reconstructed amplitude as a function of the input amplitude is presented for the measurements done with laser and for the corresponding Monte Carlo simulations. The measurements are done for the sampling and shaping time equal to approximately 60 ns. It is seen that the response of filter is linear with input signal. The error of amplitude reconstruction is presented plotting the noise figure *i.e.* the ratio (expressed in dB) between SNR at the input and output of deconvolution filter. The noise figure points (Fig. 5, right) are slightly above zero which means that there is a small degradation of SNR after the deconvolution filter. The MC simulations reproduce measurements very well. The systematic difference of the noise figure between the measurements and MC simulations is probably related to not enough precise estimation of noise in the MC simulations.

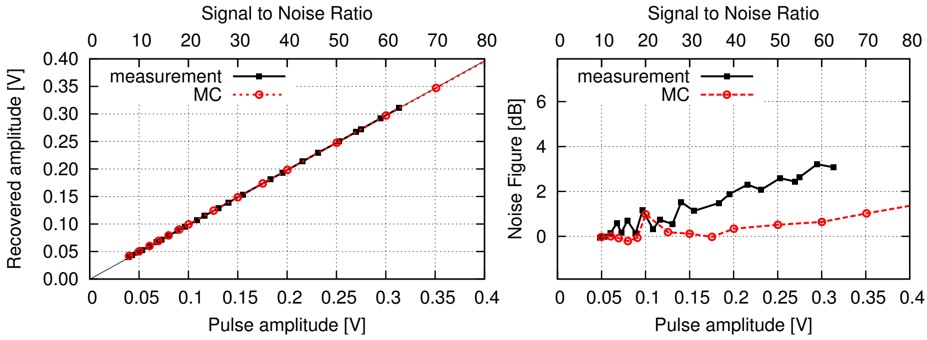

Fig. 5. Reconstructed amplitude (left) and figure of noise (right) *vs.* pulse amplitude.

Figure 6 presents the reconstructed time as a function of the input amplitude. As could be expected the reconstructed time does not depend on the amplitude. The offset between the measurements and MC simulations is due to constant delay of cables in the measurement setup. More interesting is the right plot where the error (RMS) of reconstructed time is presented which, depending on the pulse amplitude, stays within 2–7 ns. A very good agreement between the MC simulations and measurements is found.

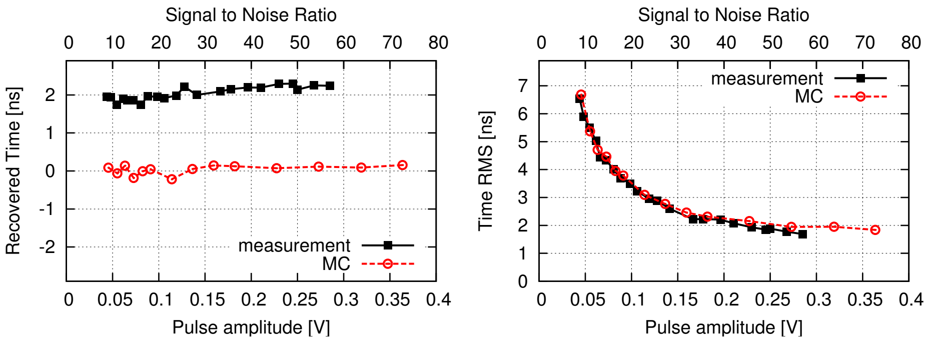

Fig. 6. Reconstructed time and its error using deconvolution algorithm.

A very important parameter in the implementation of deconvolution algorithm is the choice of sampling period. The dependence of reconstructed time and amplitude errors on the sampling period obtained with measurements and with MC simulations for the SNR = 20 is shown in Fig. 7. A very good agreement between the measurements and MC simulations is found again. For sampling periods in the range 20–40 ns the time resolution better than 2 ns is achieved. The amplitude resolution depends less on sampling period and a plateau region may be observed between 30–70 ns, for which the noise figure stays below 1 dB, *i.e.* the SNR after deconvolution is almost the same as before. One has to remember that the sampling frequency should be always a compromise between the power consumption of ADC and the requested timing resolution.

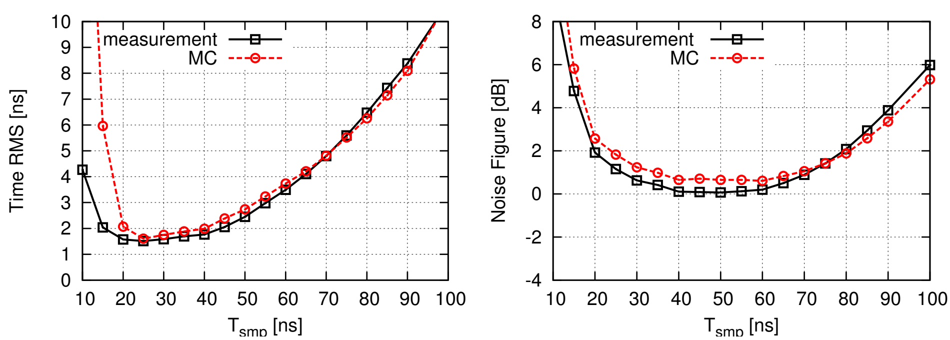

Fig. 7. Error of reconstructed time and figure of noise (SNR = 20).

The impact of pulse shape degradation on time recovery precision is presented in Fig. 8 (left) which shows the dependence of timing error on sensor bias voltage (HV). For weak electric field (low HV) the charge collection time increases and lengthens current pulse. The longer, non delta-like, pulse causes deviation from the ideal CR-RC shaping. The deteriorated pulse shape causes quantitative decrease of timing resolution. Nevertheless, the quantitative differences between the measured curves are rather small, of the order of 1 ns, what means that the method is moderately sensitive to the quality of pulse shape.

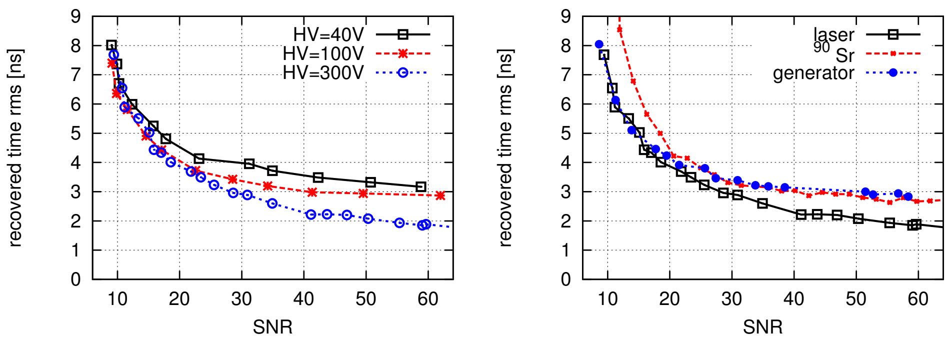

Fig. 8. Impact of sensor bias voltage (left) and signal source (right) on time recovery precision.

As a final experimental verification of deconvolution method the measurements of timing error are performed using different modes of pulse generation. In Fig. 8 (right) the standard measurements done with laser source are compared to the measurements done using ^{90}Sr radioactive source and to the measurements done with pulse generator.

A good qualitative agreement of all three curves is seen. Some quantitative differences, of the order of 1 ns, may be related to: relatively long rise time ($\gtrsim$ 2.5 ns) of input pulse for the pulse generator mode; poor timing resolution of reference photomultiplier signal and non negligible time of flight of electrons for the ^{90}Sr radioactive source mode. As already explained the measurements done with the laser are considered the most precise ones.

5. Summary

The deconvolution based reconstruction of time and amplitude information in triggerless detection system has been studied with MC simulations and verified experimentally. The measurements were performed with the whole chain of real detection system, including the dedicated front–end electronics developed for the LumiCal detector. For the given specifications, *i.e.* the CR-RC shaping with $T_{\mathrm{peak}} = 60$ ns and the SNR = 20, a precise timing information down to 1–2 ns, a good amplitude reconstruction and pileup rejection were obtained, optimising properly the sampling period. The deconvolution performed on the measured data shows very good agreement with MC simulations.

It may be concluded that the readout comprising of sensor + front–end + ADC + DSP is a very good candidate for use in triggerless systems replacing traditional dual chain readouts. A sub-nanosecond resolution may be possibly obtained using shorter shaping/sampling times or multilayer detector systems but this aspect has not been studied yet.

This work was supported by the Polish Ministry of Science and Higher Education under contract No. 1246/7.PR UE/2010/7.

REFERENCES

[1] The Compact Linear Collider Study Web Site, `http://clic-study.web.cern.ch/`

[2] M. Idzik *et al.*, The Concept of LumiCal Readout Electronics, EUDET-Memo-2007-13, `http://www.eudet.org/e26/e28`

[3] Ti. Bienz, Strangeonium Spectroscopy at 11 GeV/c and Cherenkov Ring Imaging at the SLD, PhD Thesis.

[4] S. Gadomski *et al.*, *Nucl. Instrum. Methsods* **A320**, 217 (1992).

[5] M. Idzik *et al.*, *Nucl. Instrum. Methods* **A608**, 169 (2009).

[6] G. Casinovi, R.J. Ho, Computer Generation of Colored Noise for Time-domain Analysis of Integrated Circuits, Analog Integrated Circuits and Signal Processing 11, 1996.